The Self-Assembly of Lipophilic Guanosine Derivatives in Solution and on Solid Surfaces

Giovanni Gottarelli,*[a] Stefano Masiero,[a] Elisabetta Mezzina,[a] Silvia Pieraccini,[a] Jürgen P. Rabe,*[b] Paolo Samorí,[b] and Gian Piero Spada[a]

Abstract: The self-assembly of lipophilic deoxyguanosine derivatives **1** and **2** has been studied in solution by NMR spectroscopy and ESI-MS (electrospray ionization mass spectrometry). NMR data show the existence of two types of self-assembled, ribbonlike structures (**A** and **B**), which are connected at the guanine moieties through two different H-bonded networks. The first species (**A**), which is stable in the solid state and characterised by cyclic NH(2)−O(6) and NH(1)−N(7) hydrogen bonds, is detected soon after dissolving the polycrystalline powder in rigorously anhydrous $CDCl_3$. In solution it slowly undergoes a structural transition towards a thermodynamically stable ribbon characterised by NH(1)−O(6) and NH(2)−N(3) cyclic hydrogen bonds (**B**). On the other hand, at surfaces, self-assembled ribbon nanostructures have been grown from solutions of derivative **1** both on mica and at the graphite–solution interface. They have been investigated by means of tapping mode scanning force microscopy (SFM) and scanning tunnelling microscopy (STM), respectively. SFM revealed dry, micrometer-long nanoribbons with a molecular cross-section, while STM imaging at submolecular resolution indicates a molecular packing of type **A**, like the one detected in the solid state. This indicates that, upon adsorption at the solid–liquid interface, the guanosine moieties undergo a structural rearrangement from a **B**-type to an **A**-type ribbon.

Keywords: guanine · NMR spectroscopy · scanning probe microscopy · self-assembly

Introduction

The self-assembly of small molecular units into noncovalently bonded polymeric nanostructures is a subject of continuous interest.[1–3] In particular, the self-organisation of organic molecules on flat solid surfaces gives structures with a high degree of order, thereby opening a wide range of applications, for example, in electronic and optical devices.[3–6] For a long time, the Langmuir–Blodgett technique has been employed to produce monolayers.[5] More recently, the spontaneous self-assembly of small molecules from solution directly onto solid surfaces has been used to design two-dimensionally organised structures.[1d–h, 3, 4] The hydrogen-bonded networks that can be formed between DNA bases are particularly interesting. While a lot of work has been done on unsubstituted bases,[2] the self-assembly of ribose-functionalised bases is far from being completely understood. The network formed by guanine derivatives seems particularly interesting in view of the singular electron-donor properties of the base and because lipophilic guanosine derivatives form a completely new class of lyotropic liquid crystalline phases in hydrocarbon solvents.[7]

In this paper, we report a study of the self-assembly of lipophilic guanosines **1** and **2** and the formation of planar,

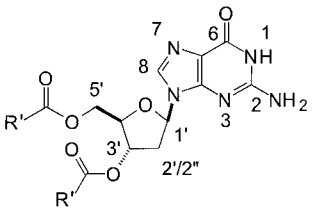

1 R' = *p*-($C_{12}H_{25}O$)C_6H_4
2 R' = C_9H_{19}

highly ordered, hydrogen-bonded networks both in dry thin films and at the solid–liquid interface. The molecular structures of these architectures were resolved by tapping mode scanning force microscopy (SFM) on mica surfaces and by scanning tunnelling microscopy (STM) at the solution–

[a] Prof. G. Gottarelli, Dr. S. Masiero, Dr. E. Mezzina, S. Pieraccini, Prof. G. P. Spada
Dipartimento di Chimica Organica "A. Mangini"
Università di Bologna
Via S. Donato 15, 40127 Bologna (Italy)
Fax: (+39)-051-244064
E-mail: gottarel@alma.unibo.it

[b] Prof. Dr. J. P. Rabe, Dr. P. Samorí
Department of Physics, Humboldt University Berlin
Invalidenstrasse 110, 10115 Berlin (Germany)
Fax: (+49)-30-20937632
E-mail: rabe@physik.hu-berlin.de

0947-6539/00/0617-3242 $ 17.50+.50/0 *Chem. Eur. J.* **2000**, *6*, No. 17

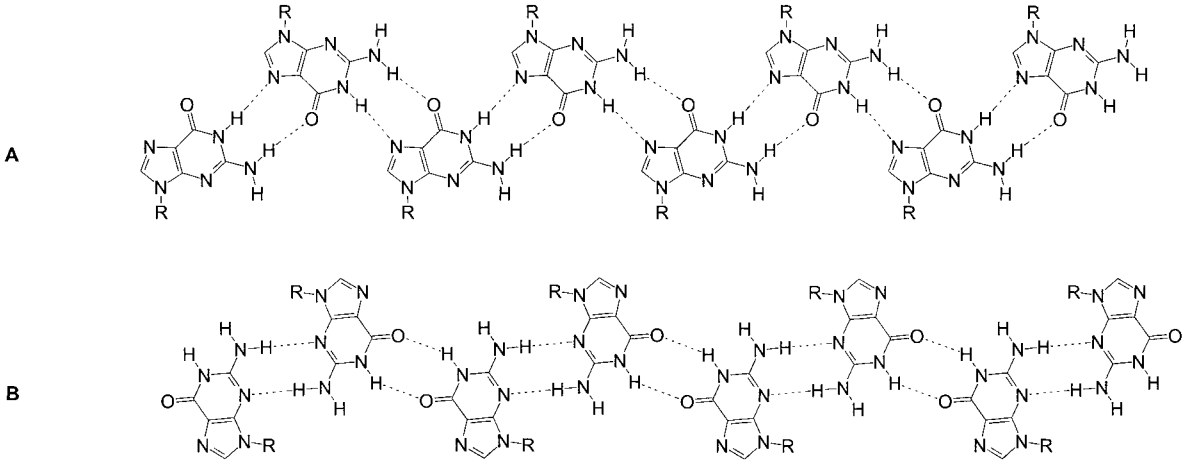

Figure 1. H-bond pattern of two possible ribbonlike assemblies of lipophilic guanosines.

graphite interface. In solution, NMR spectroscopy and ESI mass spectrometry were employed. NMR data show the existence of two assembled species. The first species is detected soon after dissolving the solid in rigorously anhydrous $CDCl_3$ and appears to be a ribbonlike structure characterised by cyclic NH(2)–O(6) and NH(1)–N(7) hydrogen bonds (Figure 1, **A**). This metastable species slowly undergoes a structural transition towards a thermodynamically stable ribbon characterised instead by NH(1)–O(6) and NH(2)–N(3) cyclic hydrogen bonds (Figure 1, **B**).

Abstract in Italian: *L'autoassemblaggio di due derivati (**1** e **2**) lipofilici della desossiguanosina è stato studiato in soluzione mediante NMR e ESI-MS (Electrospray Ionization Mass Spectrometry). I risultati NMR indicano l'esistenza di due diverse strutture a nastro (**A** e **B**), ove le basi sono interconnesse mediante due differenti schemi di legami a idrogeno. È stato possibile visualizzare la prima specie (**A**), che è stabile in fase solida ed è caratterizzata da legami a idrogeno ciclici NH(2)--O(6) e NH(1)--N(7), appena dopo averne disciolto una sua polvere policristallina in $CDCl_3$ rigorosamente anidro. In soluzione questa struttura si trasforma lentamente nel nastro termodinamicamente più stabile (forma **B**) caratterizzato da legami idrogeno ciclici NH(1)--O(6) e NH(2)--N(3). Strutture a nastro del composto **1** sono state fatte crescere da una soluzione sia su substrati di mica che all'interfaccia soluzione-grafite; queste nanostrutture sono state studiate rispettivamente con la Microscopia a Scansione di Forza (SFM), nella versione di Tapping Mode, e con la Microscopia ad Effetto Tunnel (STM). La tecnica SFM ha permesso di visualizzare in aria nanonastri con lunghezza dell'ordine dei micrometri e con una sezione dalle dimensioni molecolari, mentre la tecnica STM ha permesso di raggiungere una risoluzione sub-molecolare e di riconoscere l'aggregazione molecolare tipico della struttura a nastro **A**, analoga a quella osservata in fase solida. Questo indica che durante l'assorbimento all'interfaccia solido-liquido si osserva un riarrangiamento strutturale da un nastro di tipo **B** ad uno di tipo **A**.*

Results and Discussion

Solution studies: In previous research,[7] some of us have studied the self-assembly of the lipophilic guanosine **2** in $CDCl_3$ and in hydrocarbon solutions by NMR and IR spectroscopy and ESI-MS. It was concluded that **2** self-assembles into the ribbonlike structure **B** (Figure 1). Here, we have undertaken a similar study on derivative **1.** It revealed that, while the H(8) signal is at $\delta = 7.7$ in the NMR spectrum of **2**, the H(8) signal in the NMR spectrum of derivative **1**, dissolved in rigorously anhydrous $CDCl_3$, is found above $\delta =$ 8, independent of concentration. Moreover, the freshly prepared solution, even if diluted, displays a considerable broadening of all bands. Over a few hours, the H(8)signal moves slowly upfield and eventually reaches the "standard" value of $\delta = 7.7$. Furthermore, with dideuterotetrachloroethane as a solvent, the H(8) signal of **1** is above $\delta = 8$, but after a heating–cooling cycle the spectrum returns immediately to standard, that is H(8) signal at $\delta = 7.7$. The newly assembled form is prevalent when the H(8) signal is above $\delta = 8$, the deshielding presumably being caused by the involvement of N(7) as a proton acceptor in the self-assembling process. The presence of water in the solution increases the rate of formation of the **B** polymeric form, whose H(8) signal falls to around $\delta = 7.7$. These observations indicate that freshly prepared solutions maintain a memory of the solid state. As time passes, or after heating, a structure is achieved that is more stable in solution. We have therefore re-examined the self-assembly of derivative **2**, whose spectrum is simpler. Similarly to what was reported above for derivative **1**, a 0.03 M solution of **2** in rigorously anhydrous $CDCl_3$ shows a broad H(8) signal centred at $\delta = 8.1$ (Figure 2a). Within a few hours, the signal moves upfield and sharpens. After twelve hours it is recorded at $\delta = 7.95$ and after four days it reaches $\delta = 7.89$ (Figure 2b)). Addition of water (1 μL) finally moves the signal to $\delta = 7.7$ (Figure 2c).

The absence of two separate signals for the H(8) seems to exclude a slow equilibrium (on the NMR timescale) between two species (Figure 1). This seems to contradict the observa-

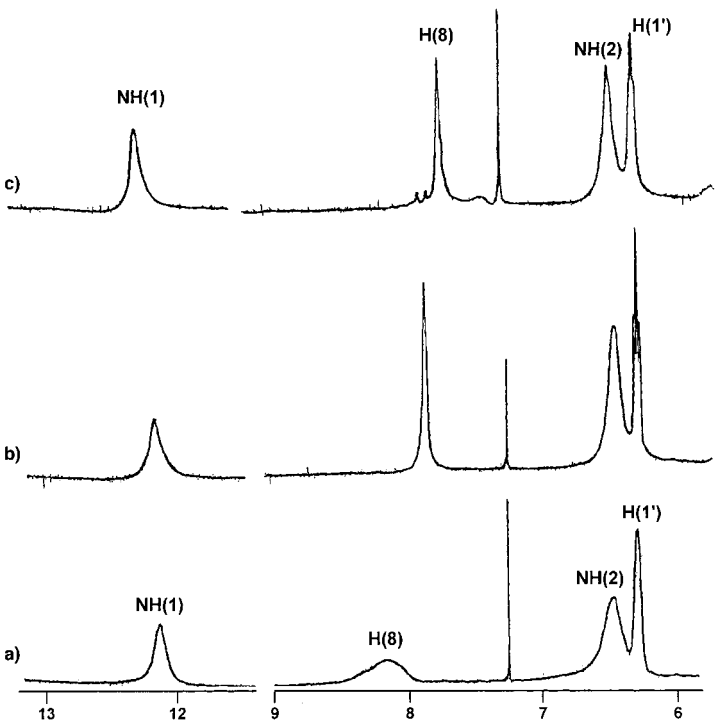

Figure 2. ^{1}H NMR spectra of derivative **2** (0.03 M in $CDCl_3$): a) immediately after dissolution, b) after four days and c) after equilibration upon addition of 1 μL water. It should be noted that in all cases, the NH(2) signals are downfield with respect to the H(1′). This indicates that this group is fully hydrogen bonded[7].

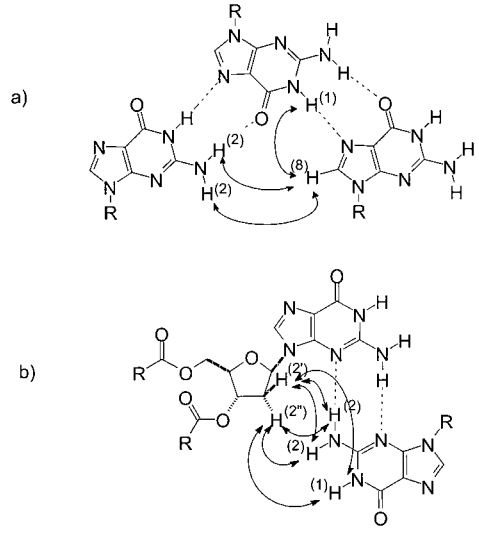

Figure 3. The NOE interaction characteristic of: a) ribbon **A** and b) **B** as indicated by double-head arrows.

tion that the transformation from **A** to **B** is slow. The two observations can be reconciled by considering a mechanism in which the first aggregate **A** rearranges through a continuous transformation, in which the proton shifts gradually change, into the more stable assembled species **B**. As the ribbonlike structure **A** was previously found in the guanosine crystal by X-ray diffraction[8] and the structure of ribbon **B** was assigned to the assembled form of derivative **2** in $CHCl_3$ solutions from an NMR study,[7] we conclude that the **A** form is present in freshly prepared $CDCl_3$ solutions.

In order to further characterise the two forms in solution, some ^{1}H-^{1}H nuclear Overhauser effect (NOE) spectra were recorded at different times. Ribbon **A** is characterised by the proximity of H(8) and NH(1) and of H(8) and NH(2) (see Figure 3a). On the other hand, the **B** form is characterised by NOE enhancements due to the proximity between H(1′), H(2′), H(2″), and the α-protons of the 3′-*O*-decanoyl group of one molecule, and NH(1) and NH(2) of the closest molecule(Figure 3b).[7, 9]. For the sake of simplicity, we are only going to consider the data obtained by irradiating H(8) (**A** form) and H(2′) and H(2″) (**B** form).

All NOE experiments recorded immediately after the dissolution of compound **2** in anhydrous $CDCl_3$ (H(8) at $\delta =$ 8.1) show significant enhancement of NH(1) (4.5%) and NH(2) (7.4%) caused by the saturation of H(8). On the other hand, the characteristic NOEs of the **B** aggregate obtained by irradiating H(2′) [(NH(1)/H(2′) and NH(2)/H(2′)] and H(2″) [(NH(1)/H(2″) and NH(2)/H(2″)] are almost negligible (<1%). The situation changes if the same NOEs are recorded after 24 hours. Saturation of H(8) gives smaller increments of NH(1) (3%) and NH(2) (5.5%). Saturation of H(2′) and H(2″) induces increased enhancement of NH(1) (4.3 and 3.8%, respectively) and of NH(2) (5.3 and 3.9%, respectively). Measurements of NOE increments carried out after three days confirm the increase in amount of structure **B** at the expense of structure **A** (even if the solution still shows small amounts of structure **A** after several days). These results indicate a transformation to the more stable structure **B**: the chemical shift value of H(8) gives a qualitative measure of the shift.

As the position of the H(8) signal is a probe for analysing the prevalent species in solution, it has been used to check the H-bond network structure of the fibre[7] obtained from slow evaporation of a solution of compound **2** in $CHCl_3$. In ref. [7], structure **B** was assigned to the ribbon present in the fibre on the basis of NMR data obtained at equilibrium. The ^{1}H NMR spectrum obtained by dissolution of the fibre in anhydrous $CDCl_3$ has a broad H(8) signal at $\delta = 8.3$, thus confirming that the fibre has the same structure as the solid (form **A**). Also in this case, the signal moves slowly upfield towards the standard $\delta = 7.7$ value. In our previous report,[7] we did not detect ribbon **A** in $CDCl_3$ solutions, consequently the small angle X-ray scattering (SAXS) of the fibre was interpreted in terms of ribbon **B**. In fact, the molecular dimensions of ribbons **A** and **B** are very similar and cannot be discriminated by SAXS.

As the NMR spectra of derivative **1** behave in a similar way, an analogous self-assembly into ribbonlike structures **A** and **B** can also be inferred for this compound.[9] The existence of dimeric and oligomeric structures for derivative **1** was confirmed by ESI mass spectrometry. This technique has been extensively used to characterise supramolecular structures based on metallic[10] and hydrogen bonds.[11] Derivative **1** was analysed in the positive-ion mode and the spectrum (see Figure 4) clearly shows the presence of protonated dimers, trimers and tetramers.

All these data indicate that derivatives **1** and **2** undergo similar self-assembly processes: in the solid state they both

0947-6539/00/0617-3244 $ 17.50+.50/0 *Chem. Eur. J.* **2000**, *6*, No. 17

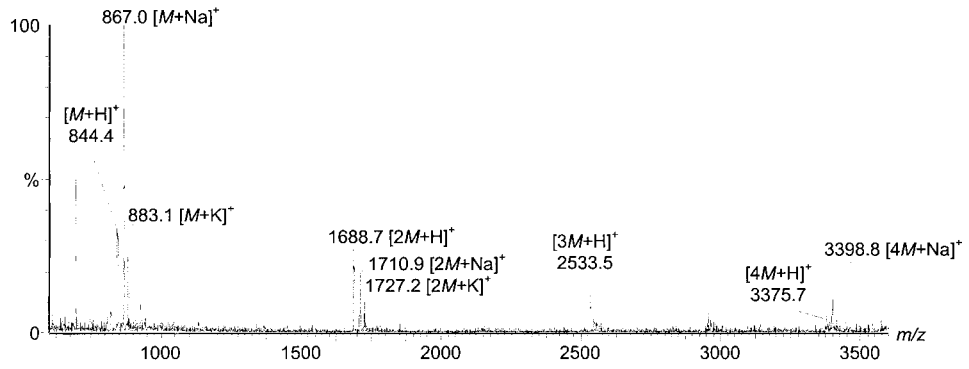

Figure 4. ESI-MS of **1** in acetone.

form **A** ribbons,[7] while in $CDCl_3$ type **B** ribbons are more stable. The microscopy investigation reported in the following paragraphs further confirm the ribbon structure.

SFM study: Guanine derivatives are known to form G quartets in the presence of metallic cations such as K^+.[12] When muscovite mica is cleaved, K^+ ions are randomly distributed on the two split surfaces.[13] It is therefore likely that the existence of these cations drives the self-assembly towards the formation of G quartets through guanine coordination with the K^+ ions.[13] In order to avoid this kind of aggregation, we have physisorbed our moieties on mica surfaces where the K^+ ions have been replaced with protons by rinsing the substrate with Millipore water and drying it under a gentle stream of N_2. By applying a drop of a 0.01M solution of **1** in 1,2,4-trichlorobenzene to the washed mica surface, it was possible to grow well-defined, dry nanoribbons on the basal plane of the substrate (Figure 5). These nanostructures are remarkably straight and exhibit a length of up to 8 μm. Their heights and widths are constant for well-defined ribbon segments, but not for the whole sample. The widths determined from single topographical profiles on SFM images need to be corrected for the broadening effect due to the finite radius of the tip. By using a model based on a rectangular cross section of the ribbon and a spherical tip, the broadening amounts to $2\Delta = 2\sqrt{h(2R-h)}$.[3] For a terminal tip radius (R) of the commercial Si tips of (13 ± 7) nm and a given height of the ribbon (h), its corrected (true) width can be evaluated. A narrow, thin type of ribbon has been monitored and is shown in Figure 5a. It is composed of different segments that have corrected widths from 6.1 nm to 6.7 nm and thicknesses from 0.95 nm to 1.1 nm. Only a very short segment of the ribbon, indicated by white arrows in Figure 5a, is 0.34 nm thick, as shown by the topographical profile in Figure 5b. Wider ribbons, like the ones in Figure 5c, have been recorded more frequently and have a true width of up to about 20 nm and a height of up to 3.2 nm. Rarely, their shape is not straight (not shown here). Another feature frequently observed is that the ribbon edges exhibit a grain. It is likely that the end of the ribbon occurs in a defined position on the substrate at which a K^+ ion has not been properly washed away and, therefore, acts as a nucleation site. It is assumed that the four guanines lie flat on the mica at this position, coordinated by the cation.

Figure 6 displays the scheme of the molecular arrangement in which the backbone is composed of bases that are connected by hydrogen bonding in positions NH(2)–O(6) and NH(1) –N(7) and the side chains are in an extended conformation. From the SFM data it is not possible to decide unambiguously whether the packing is **A** or **B** type; however, the NMR study described above points out that in the solid state ribbon **A** must be present. The width of the ribbons in this case is 6.2 nm and fits remarkably well with the narrower ribbons that have been experimentally resolved (Figure 5a).

The thickness of the aromatic moiety is 0.34 nm; hence the very short ribbon segment marked by the arrows in Figure 5a is probably made of a monolayer of guanine moieties joined by hydrogen bonds, while most of the ribbons are composed of multiple stacked layers.[7] The various thicknesses recorded suggest a stacking in the range of three to nine layers. In these molecular arrangements, it is likely that the bases and the side chains are stacked separately.

STM study: Figure 7 displays an STM image, recorded in constrant height mode, acquired in situ of monolayers of **1** at the interface between a solution of **1** in 1,2,4-trichlorobenzene and the basal surface of highly oriented pyrolitic graphite

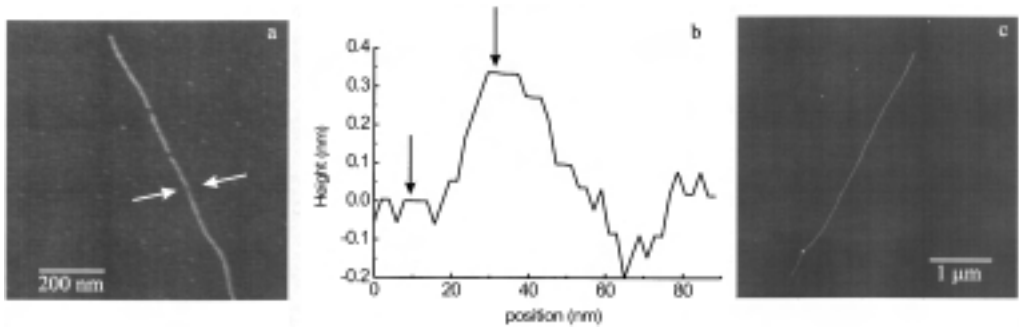

Figure 5. SFM tapping mode height images of a 0.01M solution of **1** in 1,2,4-trichlorobenzene cast on freshly cleaved, washed mica substrate. a) Ribbon with smallest cross section. b) Topographical profile between the white arrows in a) in which a small ribbon segment is located. The step height between the two black arrows is 0.34 nm. c) Wider ribbon. Height range of the images: a) 5 nm and c) 20 nm.

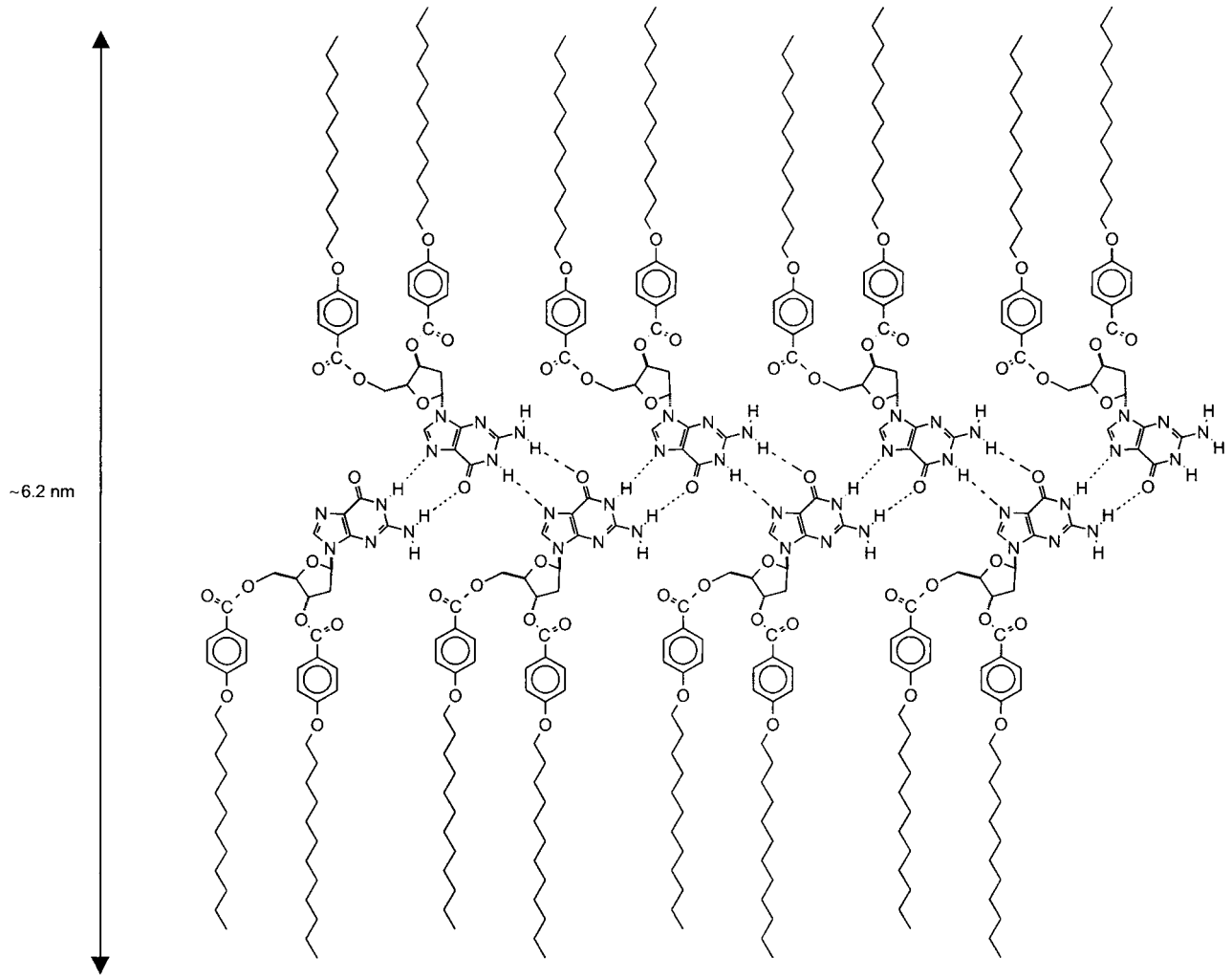

Figure 6. Scheme of the molecular arrangement of **1** in the dry ribbons visualized with SFM.

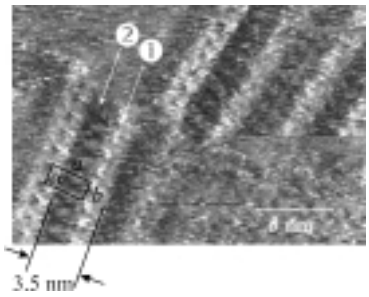

Figure 7. STM image of **1** recorded in constant height mode. The sample has been investigated at the interface between the basal plane of graphite and the organic solution ($U_t = 1.0$ V , average $I_t = 0.08$ nA). Unit cell dimensions: $a = 3.4 \pm 0.1$ nm, $b = 1.2 \pm 0.1$ nm, $\alpha = 95 \pm 4°$. White arrows indicate different contrast due to different chemical functionalities.

(HOPG). It was recorded in constant. Both the side chains and the bases lie flat on the (0001) plane of graphite, in a polycrystalline structure. Since the contrast in STM constant-height-mode imaging is mainly determined by the energy difference between the Fermi energy of the substrate and the energies of the molecular states of the adsorbate, on HOPG darker parts can generally be assigned to the aliphatic chains, characterised by a larger energy difference, and brighter parts can be ascribed to π-conjugated segments, with a smaller energy difference.[14]

A careful observation of the STM image makes it possible to discern two different parts of the molecules physisorbed at the surface (marked by white arrows in Figure 7):

1) the backbone with the bases connected by hydrogen bonding (brighter contrast),
2) the lateral substituents (black areas between 2 backbones).

The unit cell dimensions are $a = 3.5 \pm 0.1$ nm and $b = 1.2 \pm 0.1$ nm. In this case, the molecular arrangement consists of a closely packed array of hydrogen-bonded ribbons that interdigitate (Figure 8). It is worth noticing that the unit-cell dimension b perfectly matches that of ribbon **A** (1.15 nm) found in the crystals of guanosine by X-ray diffraction.[8] Therefore, ribbon **A** is probably also present at the solid–liquid interface.

It should be pointed out that the formation of a self-assembled monolayer of alkyl chains containing molecules at a solid–liquid interface requires a rather long time, typically in the order of minutes.[1e] This is due to the large number of possible states (configurations) that the system can attain. In the present case the delay time, which is the time for reaching thermodynamic equilibrium at the surface, was particularly long, that is, at least one hour. This may be attributed to the

  0947-6539/00/0617-3246 $ 17.50+.50/0 *Chem. Eur. J.* **2000**, *6*, No. 17

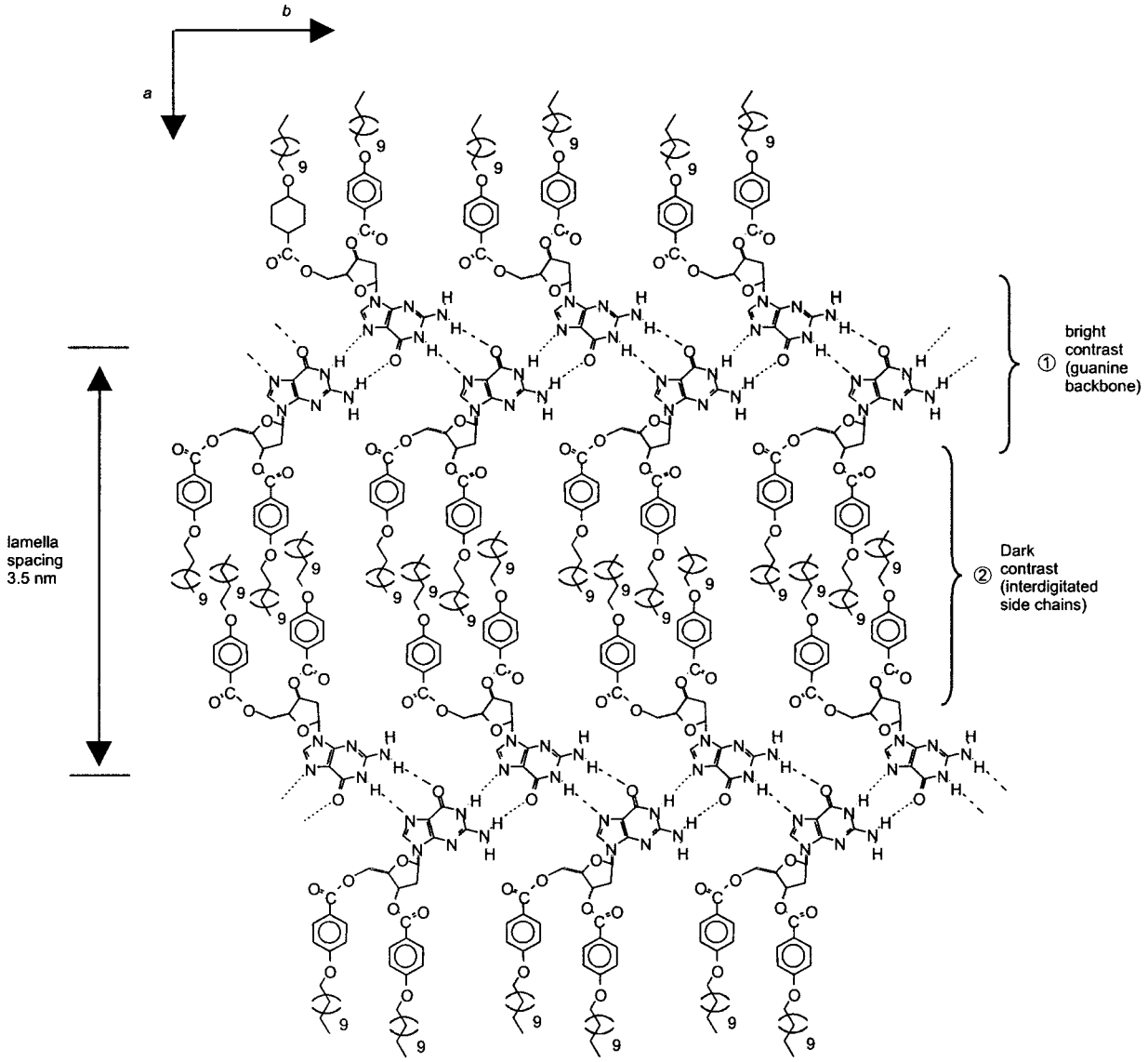

Figure 8. Scheme of the molecular packing of **1** within the lamellae. The different parts of the molecule in the hydrogen-bonded network are discerned.

fact that in solution the guanosine equilibrium state is a **B** type ribbon, while upon adsorption to the surface, a transition to the **A** type needs to take place.

Conclusion

The self-assembly of hydrogen-bonded networks of a lipophilic guanosine derivative can be used to design highly ordered supramolecular structures not only in the crystal, but also at solid surfaces and in solution. On a mica surface, micrometer-long nanoribbons with a molecular cross section have been grown, while at the interface between graphite and the organic solution, a two-dimensional polycrystalline structure has been obtained. This latter structure reflects the supramolecular architecture that has been detected both in the single crystal[8] and as a metastable state in solution by NMR spectroscopy. The possibility of producing well-defined and highly ordered guanine supramolecular structures like the ribbons presented here may be of interest for the fabrication of molecular nanowires within the framework of future molecular electronics applications.

Experimental Section

Synthesis: Derivative **2** was prepared as described in ref. [12c]. A powder was obtained from anhydrous acetonitrile. Large "quasi" crystals of derivative **2** were grown by slow evaporation of a saturated solution of **2** in $CHCl_3$ at 4 °C. The crystals had the same shape as those used for the fibre X-ray work of ref. [7].

Derivative **1** was prepared analogously in three steps starting from commercially available 2-deoxyguanosine monohydrate (Fluka). The nucleoside was converted into 9-fluoroenylmethyoxycarbonyl-dG.[15] The N-protected nucleoside (0.5 g, 1 mmol) was then treated with 4-dodecyloxybenzoyl chloride (0.81 g, 2.49 mmol) in dry pyridine (10 mL) overnight. The reaction mixture was diluted with CH_2Cl_2 and washed with saturated $NaHCO_3$. The organic layer was concentrated in vacuo. Traces of pyridine were removed by coevaporation with toluene. The crude material thus obtained was purified by column chromatography on silica with CH_2Cl_2/MeOH 97:3 as the eluant, to afford the N-protected diester as a spongy solid in a 68% yield. ^{1}H NMR ($CDCl_3$): $\delta = 0.80-0.95$ (m, 6H), 1.15–1.50 (m, 36H), 1.70–1.85 (m, 4H), 2.70–2.90 (m, 1H), 3.15–3.30 (m, 1H),

3.85 – 4.10 (m, 4H), 4.28 (t, 1H), 4.49 (d, 2H), 4.58 – 4.90 (m, 3H), 5.80 – 5.85 (m, 1H), 6.50 (t, 1H), 6.75 – 7.00, 7.20 – 7.40, 7.55 – 8.25 (3m 17H), 9.10 (brs, 1H), 11.30 (brs, 1H).

The N-protected diester (0.15 g, 0.14 mmol) was converted into the target derivative **1** by reaction (2 h) with piperidine (0.7 mL) in CH_2Cl_2 (20 mL). The reaction mixture was washed with saturated $NaHCO_3$ and bidistilled water, and concentrated in vacuo. Purification by column chromatography on silica gel (eluant: gradient from CH_2Cl_2/MeOH 97:3 to CH_2Cl_2/MeOH 95:5) afforded derivative **1** in a 65% yield as a colourless glassy material. ^{1}H NMR ($CDCl_3$): $\delta = 0.75 - 0.90$ (m, 6H), 1.10 – 1.50 (m, 36H), 1.60 – 1.85 (m, 4H), 2.60 – 2.75 (m, 1H), 2.90 – 3.10 (m, 1H), 3.90 – 4.05 (m, 4H), 4.55 – 4.80 (m, 3H), 5.65 – 5.75 (m, 1H), 6.10 – 6.35 (m, brs, 3H), 6.90 (m, 4H), 7.72 (s, 1H), 7.98 (m, 4H), 12.10 (brs, 1H). ^{13}C NMR ($CDCl_3$): $\delta =$ 14.10 ($2CH_3$), 22.68 (CH_2), 26.00 (CH_2), 29.13 (CH_2), 29.16 (CH_2), 29.19 (CH_2), 29.22 (CH_2), 29.36 (CH_2), 29.40 (CH_2), 29.43 (CH_2), 29.46 (CH_2), 29.65 (CH_2), 31.92 (CH_2), 37.36 (CH_2), 63.90 (CH_2), 68.27 (CH_2), 68.35 (CH_2), 75.08 (CH), 82.73 (CH), 84.52 (CH), 114.26 (CH), 114.53 (CH), 117.81 (C), 121.32 (C), 121.56 (C), 131.72 (CH), 131.80 (CH), 135.73 (CH), 151.42 (C), 153.66 (C), 159.06 (C), 163.28 (C), 163.48 (C), 165.57 (C), 166.02 (C).

Scanning force microscopy: Dry samples were prepared by solution casting. A drop of a very diluted solution of **1** in 1,2,4-trichlorobenzene (concentrations between 0.01 and 0.001 g L^{-1}) was placed onto a freshly cleaved muscovite mica disc (Plano W. Plannet GmbH). Crystallisation takes place upon the evaporation of the solvent. The organic solution was cast on bare, freshly cleaved mica, rinsed with Millipore water. We chose 1,2,4-trichlorobenzene (Aldrich) as solvent because of its high boiling point (214 °C), which slows down the molecular physisorption process. The samples were stored at room temperature and pressure, sealed inside a Petri dish, for about 72 hours. The sample surfaces were studied by tapping mode scanning force microscopy (SFM).[16, 17] Experiments were carried out in air at room temperature with a Nanoscope IIIa.[18] The height signal (output of the feedback signal) was recorded with a scan rate of 1 – 3 lines s^{-1} and a lateral resolution of 512×512 pixels. Microfabricated silicon nanoprobes (length 125 μm and width 30 μm) with a spring constant between 17 and 64 N m^{-1}[18] were used. The piezo, with a maximum $x-y$ scan range of 15.3 μm, was calibrated routinely in all three dimensions by imaging gold and mica surfaces. The scan range between 15.3 μm and 0.5 μm was explored. Surface profiles and dimensions of the visualized ribbons were estimated by using the software of the Nanoscope apparatus.

Scanning tunnelling microscopy: The STM investigation at the solid – liquid interface[1d] was carried out with a homemade, low-current, beetle-type scanning tunnelling microscope.[3] First, the HOPG lattice (Advanced Ceramics Corp, grade ZYH) was visualized for a few hours until a thermal equilibrium (absence of mechanical drift of the system) was reached. A drop of an almost saturated solution of **1** in 1,2,4-trichlorobenzene, prepared more than one week before, was applied to the basal plane of the substrate. Then the Pt/Ir electrochemically etched tip was immersed in the organic solution. By varying the tunnelling parameter, it was possible either to observe the first organic layer that was physisorbed on the basal plane of the conductive substrate, or to visualize the lattice of the HOPG substrate underneath. This allowed the calibration of the piezo to be accomplished in situ.

Spectroscopy experiments: ^{1}H Spectra and ^{1}H-^{1}H NOE measurements were carried out with a Varian Gemini 300 instrument; δ(H) are in ppm from the solvent peak in $CDCl_3$ solutions. In NOE experiments, a number of transients (1024 – 2048) were accumulated by using relaxation delays of 1 – 3 s and a minimum decoupler power to obtain NOE signals. The instrumental settings were: spectral width 4.5 kHz, pulse width 12 μs (90° flip angle). ESI-MS spectra were obtained in acetone or in methanol (0.1 – 0.5 mg mL^{-1}) with a Waters Platform ZMD 4000 (courtesy of Dr. Roberto Coldani, Waters SpA, Italy). No special care was taken to eliminate traces of alkali metal ions.

Acknowledgements

We thank the University of Bologna (funds for selected research topics 1997 – 99) and MURST (National Program: Structure, Order, Dynamics and Applications of Liquid crystalline Systems; Cofin '99) for financial support and Dr. Roberto Coldani (Waters SpA, Italy) for ESI-MS experiments. Research in Berlin on the self-assembly of molecular nanostructures is supported by the EU-TMR project SISITOMAS. P.S. acknowledges the EU for a TMR grant.

[1] For some recent examples see: a) R. P. Sijbesma, F. H. Beijer, L. Brunsveld, B. J. B. Folmer, J. H. K. K. Hirschberg, R. F. M. Lange, J. K. L. Lowe, E. W. Meijer, *Science* **1997**, 278, 1601 – 1604; b) H. A. Klok, K. A. Jolliffe, C. L. Schauer, L. J. Prins, J. P. Spatz, M. Möller, P. Timmermann, D. N. Reinhoudt, *J. Am. Chem. Soc.* **1999**, 121, 7154 – 7155; c) W. Yang, X. Chai, L. Chi, X. Liu, Y. Cao, R. Lu, Y, Jiang, X. Tang, H. Fuchs, T. Li, *Chem. Eur. J.* **1999**, 5, 1144 – 1148; d) J. P. Rabe, S. Buchholz, *Science* **1991**, 253, 424 – 427; e) P. Bäuerle, T. Fischer, B. Bidlingmeier, A. Stabel, J. P. Rabe, *Angew. Chem.* **1995**, *107*, 335 – 339; *Angew. Chem. Int. Ed. Engl.* **1995**, *34*, 303 – 307; f) K. Eichhorst-Gerner, A. Stabel, G. Moessner, D. Declerq, S. Valiyaveettil, V. Enkelmann, K. Müllen, J. P. Rabe, *Angew. Chem.* **1996**, *108*, 1599 – 1602; *Angew. Chem. Int. Ed. Engl.* **1996**, *35*, 1492 – 1495; g) S. De Feyter, P. C. M. Grim, M. Rücker, P. Vanoppen, C. Meiners, M. Sieffert, S. Valiyaveettil, K. Müllen, F. C. De Schryver, *Angew. Chem.* **1998**, *110*, 1281 – 1284; *Angew. Chem. Int. Ed.* **1998**, *37*, 1223 – 1226; h) M. S. Vollmer, F. Effenberger, R. Stecher, B. Gompf, W. Eisenmenger, *Chem. Eur. J.* **1999**, *5*, 96 – 101.

[2] For recent studies of self-assembled DNA bases on graphite; for adenine see: a) T. Uchihashi, T. Okada, Y. Sugawara, K. Yokoyama, S. Morita, *Phys. Rev. B* **1999**, *60*, 8309 – 8313; for guanine see: b) S. J. Sowerby, M. Edelwirth, W. Heckl, *J. Phys. Chem. B* **1998**, *102*, 5914 – 5922.

[3] P. Samorí, V. Francke, K. Müllen, J. P. Rabe, *Chem. Eur. J.* **1999**, *5*, 2312 – 2317.

[4] L. A. Bumm, J. J. Anrold, M. T. Cygan, T. D. Dunbar, T. P. Burgin, L. Jones II, D. L. Allara, J. M. Tour, P. S. Weiss, *Science* **1996**, *271*, 1705 – 1707.

[5] A. Ulman, *An Introduction to Ultrathin Organic Films*, Academic Press, London, **1991**.

[6] R. H. Friend, R. W. Gymer, A. B. Holmes, J. H. Burroughes, R. N. Marks, C. Taliani, D. D. C. Bradley, D. A. Dos Santos, J. L. Brédas, M. Lögdlund, W. R. Salaneck, *Nature* **1999**, 397, 121 – 128.

[7] G. Gottarelli, S. Masiero, E. Mezzina, G. P. Spada, P. Mariani, M. Recanatini, *Helv. Chim. Acta* **1998**, *81*, 2078 – 2092.

[8] U. Thewalt, C. E. Bugg, R. E. Marsh, *Acta Crystallogr. Sect. B* **1970**, *26*, 1089 – 1101.

[9] At equilibrium, the δ value of the NH(2) shifts downfield with concentration indicating progressive engagement in H-bonding, just as in the case of derivative **2**[8].

[10] B. Hasenknopf, J. M. Lehn, M. Boumediene, A. Dupont-Gervais, A. Van Dorsselaer, B. Kneisel, D. Fenske, *J. Am. Chem. Soc.* **1997**, *119*, 10956 – 10962.

[11] C. A. Shalley, R. K. Castellano, M. S. Brody, D. M. Rudkevich, G. Siazdak, J. Rebek, Jr., *J. Am. Chem. Soc.* **1999**, *121*, 4568 – 4579.

[12] a) J. M. Williamson, *Curr. Opin. Struct. Biol.* **1993**, *3*, 357 – 362; b) C. T. Marsh, J. Vesenka, E. Henderson, *Nucleic Acids Res.* **1995**, *23*, 696 – 700; c) G. Gottarelli, S. Masiero, G. P. Spada, *J. Chem. Soc. Chem. Commun.* **1995**, 2555 – 2557; d) V. Andrisano, G. Gottarelli, S. Masiero, E. H. Heijne, S. Pieraccini, G. P. Spada, *Angew. Chem.* **1999**, *111*, 2543 – 2544; *Angew. Chem. Int. Ed.* **1999**, *38*, 2386 – 2388; e) A. Marlow, E. Mezzina, S. Masiero, G. P. Spada, J. T. Davis, G. Gottarelli, *J. Org. Chem.* **1999**, *64*, 5116 – 5123.

[13] S. Nishimura, P. J. Scales, H. Takeyama, K. Tsunematsu, T. W. Healy, *Langmuir* **1995**, *11*, 291 – 295.

[14] R. Lazzaroni, A. Calderone, J. L. Brèdas, J. P. Rabe, *J. Chem. Phys.* **1997**, *107*, 99 – 105.

[15] L. H. Koole, H. M. Moody, N. L. H. L. Broeders, P. J. L. M. Quaedflieg, W. H. A. Kuijpers, M. H. P. van Genderen, A. J. J. M. Coenen, S. van der Wal, H. M. Buck, *J. Org. Chem.* **1989**, *54*, 1657 – 1664.

[16] C. Bustamante, D. Keller, *Physics Today* **1999**, *48*, 32 – 38.

[17] J. Tamayo, R. Garcia, *Langmuir* **1996**, *12*, 4430 – 4435.

[18] Nanoscope III Multimode, Digital Instruments, Santa Barbara, CA.

Received: December 20, 1999 [F2195]

  0947-6539/00/0617-3248 $ 17.50+.50/0